Recognition of Shapes for Object Retrieval in Image Databases by Discrete Curve Evolution and Two Consecutive Primitive Edges

Tian-Luu Wu and Ji-Hwei Horng

Abstract- **This paper presents the recognition of shapes for object retrieval in image databases using skeleton-based and contour-based representation by discrete curve evaluation and two consecutive primitive edges. Humans tend to use high-level concepts in everyday life. Object segmentation and recognition is the primary step of computer vision to achieve image retrieval of high-level image analysis. Contour-based and skeleton-based representations are important for object recognition in different areas. In comparing the contour-based approaches with the skeleton-based approaches for object representation, the contour-based is more sensitive to noise than a skeleton-based approach based on a good skeleton pruning method, but a rough shape classification can be performed since the obtained skeletons do not represent any shape details. In this paper, we proposed a novel method to integrate the contour-based approaches with skeleton-based approaches for object representation. The contour-based and skeleton-based representations are based on the proposal of two consecutive primitive edges method and discrete curve evolution method respectively. Experimental results demonstrate that the performance of the proposed algorithm is superior to Torsello and Hancock's method [7] in terms of retrieval accuracy.**

Index Terms: Keywords: Skeleton, shape similarity measure, visual parts, discrete curve evolution

I. INTRODUCTION

In the past, contour and skeleton were usually used to analyze and represent the shape of objects. Contour-based is an important aspect of human visual perception. Polygonal approximation has been a very popular shape representation technique. It not only satisfactorily represents a shape, but also significantly reduces the amount of processing data for further applications. Therefore, many shape recognition (matching) methods through polygonal approximation [1] have been proposed. However, some conventional methods are somewhat sensitive to non-consistent results of polygonal approximation. For example, the method [1] using attributed string matching cannot accurately define the edit distance (cost) for insertion and deletion operations. Latrcki and Lakamper [2] proposed a convexity rule for shape decomposition based on discrete contour evolution. They concentrate some of decomposition of *2D* objects into meaningful visual parts and proposed a contour evaluation method for identifying the visual part whether it is a significant convex part or not.

The skeleton is another important method for object representation and recognition. Skeleton-based representations are the abstractions of objects, which contain both shape features and topological structures of original objects. Many researchers have made efforts to recognize the generic shape by matching skeleton structures represented by graphs or trees [3]. Unfortunately, these approaches have only demonstrated the applicability to objects with simple and distinctive shapes, and therefore, cannot be applied to more complex shapes like shapes in a MPEG-7 data set.

The most common approaches for overcoming skeleton instability are based on skeleton pruning. Pruning can either be performed implicitly as a post processing step or integrated in the step of skeletonization computation. In general, the skeletonization algorithms can broadly be classified into four types: (1) the first type is thinning algorithms, such as those with shape thinning and the wave front/grassfire transform. These algorithms iteratively remove border points, or move to the inner parts of an object in determining an object's skeleton; (2) the second type is the category of discrete domain algorithms based on the Voronoi diagram. These methods search the locus of centers of the maximal disks contained in the polygons with vertices sampled from the boundary; (3) the third type of algorithms is to detect ridges in a distance map of boundary points. Approaches based on distance maps usually ensure accurate localization but does not guarantee that the skeleton can connect completely; (4) the fourth type of algorithms is based on mathematical morphology. Usually, these methods can localize the accurate skeleton, but may not guarantee the connectivity of the skeleton.

In this paper, we proposed a method to integrate the contour-based approaches with skeleton-based approaches for object representation. The contour-based and skeleton-based approaches are based on the proposed two consecutive primitive edges method and the discrete curve evolution method respectively. To overcome skeleton instability based on skeleton pruning, the proposed skeleton pruning approaches can prune the redundant skeleton branches based on the contour estimation and pre-selection of the implicit skeleton branches.

II. SKELETON GROWING WITH CONTOUR INFORMATION

A. The Proposed Contour Sampling Method using Discrete

Manuscript received January 3, 2009.

Tian-Luu Wu is with the Electronic Engineering, National Kinmen Institute of Technology, Taiwan, R.O.C. (corresponding author to provide phone: +886-82-313559; fax: +886-82-313304; e-mail:wtlu@kmit.edu.tw).

Ji-Hwei Horng is with the Electronic Engineering, National Kinmen Institute of Technology, Taiwan, R.O.C. (e-mail:horng@kmit.edu.tw).

Curve Evolution

GHT [4] was initially proposed to represent a planar set *D* with arbitrary boundary using a so-called *R*-table [4]. As an example shown in Fig. 1, the boundary of the planar set *D* can be described by geometric relationship between the centroid X^R of *D* and the boundary point *X*'s. According to the *R*-table in GHT to represent the boundary in question can be constructed as:

$$\begin{aligned}
&\phi_1(r_1^1,\alpha_1^1),(r_1^2,\alpha_1^2),...,(r_1^{n1},\alpha_1^{n1}),\\
&\phi_2(r_2^1,\alpha_2^1),(r_2^2,\alpha_2^2),...,(r_2^{n1},\alpha_2^{n1}),\\
&\phi_3(r_3^1,\alpha_3^1),(r_3^2,\alpha_3^2),...,(r_3^{n3},\alpha_3^{n3}),\\
&\quad\vdots\\
&\phi_k(r_k^1,\alpha_k^1),(r_k^2,\alpha_k^2),...,(r_k^{n3},\alpha_k^{n3}).
\end{aligned} \tag{1}$$

where ϕ_i is the common slope for the tangent line passing through the boundary points $x_i^j, j=1,...,n$. However, the information of *R*-table in GHT cannot link information of boundary into the planar set *D* in an image, and it is also difficult to express which boundary is a significant visual part.

The characters of significant visual part in a contour have be proposed in literature [5]. We can summarize the observation into four rules:

(1) These visual parts are defined to be "convex" or "nearly convex shape" from the rest of object at concavity extrema.
(2) Although the observation that visual parts are "nearly convex shapes" is very natural. The main problem is to determine the meaning of "nearly" in this context.
(3) Many significant visual parts are not convex in the mathematic sense, since a visual part may have small concavities, e.g., small concavities caused by fingers of the human hand.
(4) The role of each visual part in any object is different from the sense of human vision, e.g., the perpendicular angle is less than the straight line in a square shape. If the perpendicular angle is loss then it cannot form a square. On the opposite view, increasing or decreasing the straight lines, will still maintain the square. In this respect, the smaller number of visual parts is more significant than the larger number of visual parts.

To estimate the "significant" visual part in a whole object is a difficult task without a prior knowledge about the boundary of objects or without user interactive. Our solution is using a hierarchical evolution rule which includes two stages: (1) estimate the turning point of visual parts based on the chain-code method and discrete curve evolution; (2) select the visual part into significant visual parts from all of visual parts in an object.

First, we propose a contour sampling method for estimating the turning point of visual parts based on chain-code method. In the chain-code process, the point coded moves along the digital curve or edge pixels with 8-adjacency model in *8*-direct code. This assumes that the chain-code with *8*-adjacency in a *3×3* block is limited to a multiple of 45^0 and it is quantized to be the nearest multiple of 45^0. A boundary chain starts with a random point in the edge pixels. Each edge pixel has 8 neighboring points among which there is at least one edge point. The boundary chain-code is the direction description of current point a_j to the next one a_{j+1}, and the chain-code can be defined as

$$e_j = a_j \rightarrow a_{j+1} \tag{2}$$

where e_j denotes the number *0* to *7* for a description in 8-direction chain-code.

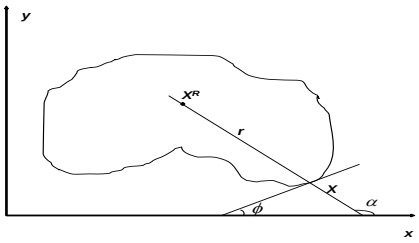

Fig. 1.The coordinated relationship between a boundary point *X* and the centroid X^R of an object with arbitrary shape.

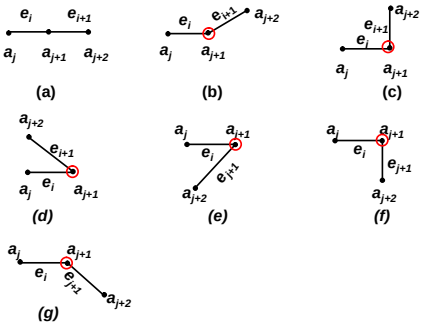

Fig.2 shows the possible *7* types of visual parts in a 3×3 block.

The boundary in a planar set *D* can be described with a start point and a series of sequence direction codes. There are some problems of chain-code method: (1) the chain-code varies dramatically with different start points. Selecting the proper start point on the chain-code is a common process; (2) the chain-code method cannot be applied to the rotation and scaling of *D*. Based on this reason, the consecutive primitive edge is proposed to describe the boundary of *D*. The concept of consecutive primitive edge ϕ_i is as follows:

$$\phi_i = | e_i - e_{i-1} |, i = 1,...,n \tag{3}$$

where e_i and e_{i-1} denote the consecutive primitive edges respectively. The detected of ϕ_i can be mapped to *7* types of visual parts, as shown in Fig.2. According to the key property of discrete curve evolution, a relevance measure *k* is given by

$$k(e_j, e_{j+1}) = \frac{\beta(e_j, e_{j+1})\ell(e_j)\ell(e_{j+1})}{\ell(e_j)+\ell(e_{j+1})} \tag{4}$$

where e_j and e_{j+1} is a pair of consecutive primitive edges, $\beta(e_j, e_{j+1})$ is the turn angle at the common vertex of primitive edge e_j and e_{j+1}, and ℓ is the length function normalized with respect to total length of the polygonal curve. The main property of this relevance measure is that the higher the value of $k(e_j, e_{j+1})$ the larger the contribution to the shape

of the curve of arc $e_j \cup e_{j+1}$. Based on satisfying the rule (1-3) mentioned above, the turning point of visual part may appear as a (red) circle in Fig. 2 using the relevance measure *k*.

The next problem is to find the significant visual part which hides in the boundary of an object. Mapping the consecutive primitive edge to a visual part is to encode an object with visual parts block by block along the boundary pixels. Hence, two given object blocks from along the edge pixel can be encoded and indicate which visual part is mapped, and the front of visual part e_{j+1} and the rear of visual part e_j in Eq. (3) are overlapping. Without loss of generality, the histogram of consecutive primitive edge is used to describe the boundary of objects in this paper. Let $CPE_i, i = 1,...,7$ denote the type of consecutive primitive edges and N_i is the number of CPE_i in Fig. 2. The boundary of object *BO* will be described by

$$BO = \sum_{1 \le k \le 7} N_k \tag{5}$$

For the *CPE*, the local significance of a boundary point is usually only considered and the global information of shape in an object is discarded. Assume that the arrangement of N_k in descending order ($N_1 \le N_2 \le N_3 \le ... \le N_7$) associates the same ordering to the CPE_is

$$CPE_1 \le CPE_2 \le,...,\le CPE_7 \tag{6}$$

A ratio is decided to reserve how much of the visual parts can represent the object as the significant visual parts and the remainder will be ignored. The ratio ρ is defined by

$$\rho \le \frac{\sum_{1 \le i \le p} N_i}{\sum_{1 \le j \le 7} N_j} \tag{7}$$

where *p* (p<7) denotes preceding sequences in eq. (7). It is important to determine a good stop criterion of the ratio selected. However, the ratio ρ selected usually appears in a variety of application-dependent cases. According to the experimental results, it can preserve the perceptual appearance sufficiently for object recognition when the ratio ρ is assigned as 0.1.

A skeleton similarity measure is useful for object-based retrieval in image databases should be according to our perception. This basic property leads to the following requirements:

(1) A skeleton similarity measure shall permit recognition of perceptually similar objects that are not mathematically identical.
(2) It shall preserve significant visual parts of objects.
(3) It shall not depend on scale, orientation, or position of objects.
(4) A skeleton similarity measure is universal, in the sense that it allows us to identify or distinguish objects of arbitrary skeleton, i.e. no restrictions on shapes are assumed.

We should further introduce the skeleton growing based on following rules.

Rule 1. Let the boundary ∂D of a set *D* be composed of *k* simple contour segments $C_1, C_2, \ldots, C_k$. Let $T_1, T_2, \ldots, T_n$ be the turning points lying on the simple contour segment, which were selected using Eq. (7). The turning point set T_i also generated a skeleton branch.

Rule 2. Besides the turning point, we should find the pruning point set P_j from the curve of plane between the neighbors of two turning points according to the average curvatures. The pruning point is used to determine the skeleton point and not to bring on the skeleton branch. The centroid $\overline{\upsilon}$ of boundary feature space is defined as:

$$(\bar{x}, \bar{y}) = (\frac{1}{N}\sum_{i=1}^{N} x_i, \frac{1}{N}\sum_{i=1}^{N} y_i) \tag{8}$$

where x_i and y_i are two-stimulus position values of *i*th vector of boundary feature spaces. Assume that function *f* denotes a curve of a plane which is composed of *n* points $c_1, c_2, \ldots, c_n$ and a point c_i at the function *f* can be represented as $(x, f(x))$ shown as Fig. 3, the curvature of c_i is

$$\Omega_i = \frac{f''(x)}{(1+f'(x)^2)^{3/2}} \tag{9}$$

the average of curvatures is computed as

$$\chi_T = \frac{\Omega_1 + \Omega_2 + ... + \Omega_n}{N_n} \tag{10}$$

the pruning point should be found as

$$|\Omega_i - \Omega_{i+1}| \ge \chi_T \tag{11}$$

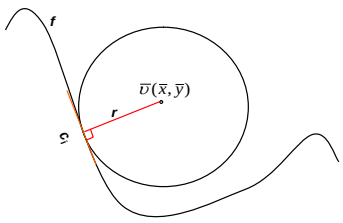

Fig. 3 shows the curvature Ω of a point c_i at the function *f*.

Rule 3. If a straight boundary is between the neighbors of two turning points, then the pruning point is determined using the center of the straight boundary.

Rule 4. The skeleton should be grown according to the boundary points set $\Re$ of the object, which include turning points set T_i and pruning points set P_j, and defined as $\Re = \{\{T_i\} \cup \{P_j\}\}, i = 1,...,n, j = 1,...,m$.

Rule 5. Connect skeleton points which are found using the boundary point set $\Re$ and turning points T_i's, the skeleton arc of the object is found.

B. Skeleton Growing

Assume that a_{i-1}, a_i, and a_{i+1} denote two consecutive points, and the a_i is a turning point which belongs to the set of T_i. The boundary segments between a_{i-1} and a_i, and a_i and a_{i+1} can be represented as $ax+by+c=0$ and $dx+ey+f=0$, respectively, where *a*, *b*, *c*, *d*, *e*, and *f* denote the parameters of boundary segments. It should find the auxiliary line *L* which connects point a_{i-1} and a_{i+1} shown as Fig.4. Let θ denote an included angle between the line $ax+by+c=0$ and $dx+ey+f=0$. That is

$$\theta = \theta_1 - \theta_2 \tag{12}$$

According to the tangent function, it can be found as

$$\tan\theta = \tan(\theta_1 - \theta_2) = \frac{\tan\frac{\theta}{2} + \tan\frac{\theta}{2}}{1 - \tan\frac{\theta}{2}\tan\frac{\theta}{2}} \quad (13)$$

Let $x = \tan\frac{\theta}{2}$, it will be computed as

$$x = \tan\frac{\theta}{2} = \frac{-(ad+be)+2(bd-ae)}{(bd-ae)} \quad (14)$$

According to the $\theta_1 = \theta_\phi + \frac{\theta}{2}$, it is simple to prove

$$\tan\theta_\phi = \tan(\theta_1 - \frac{\theta}{2}) = \frac{\tan\theta_1 - \tan\frac{\theta}{2}}{1+\tan\theta_1\tan\frac{\theta}{2}} \quad (15)$$

The straight line L_1 is found which connected the turning point and skeleton point as

$$(y - y_1) = \tan\theta_\phi (x - x_1) \quad (16)$$

The straight line L_1 should intersect another line L_2 in the object. Let the L_2 define as

$$gx+hy+i=0 \quad (17)$$

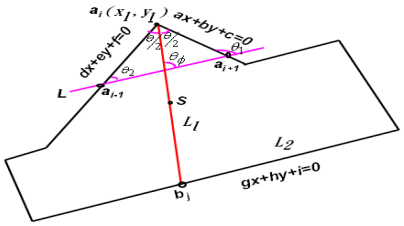

Fig. 4. A skeleton point *s is* grown using the turning point a_i.

Combining the equations (16) and (17), it is assumed that the homogeneous system has a nontrivial solution. The nontrivial solution of system should be found by performing of Guass-Jordan reduction procedure on the augmented matrix [M|0]. The result is

$$\begin{bmatrix} 1 & 0 & k_1 \mid & 0 \\ 0 & 1 & k_2 \mid & 0 \end{bmatrix} \quad (18)$$

where k_i,i=1,2 are the ratios of x and y. Based on the reduction results, the values of x_2 and y_2 has the intersect point between straight line L_1 and L_2, and can be computed as

$$(x_2, y_2) = (\frac{k_1}{\sqrt{1+k_1^2+k_2^2}}, \frac{k_2}{\sqrt{1+k_1^2+k_2^2}}) \quad (19)$$

The skeleton point should be found as

$$s = (\frac{x_1+x_2}{2}, \frac{y_1+y_2}{2}) \quad (20)$$

Based on the skeleton point sets s_k, $k = n+m$ is found from the boundary points set $\Re$ of the object. The skeleton arc comes into being according to the following algorithm.

Algorithm 1: Proposed the skeleton arc of object comes into being.

Input: Two boundary point sets $\{T_i\}$ and $\Re = \{\{T_i\} \cup \{P_j)\}, i = 1,...,n,\ j = 1,...,m$

Output: A skeleton arc of the object comes into being.

Method:

1. Let *S* denote the collection of all the skeleton point sets s_k, and empty initially.
2. Let *E* denote the completed skeleton arc of an object and empty initially.
3. while $(\Re \neq NULL)$
   Find a skeleton point using a boundary point in $\Re$ by the equation (20).
   Insert the skeleton point into *S* and delete the skeleton point from $\Re$.
4. Select a skeleton point from *S* to *E*.
5. While $(S \neq NULL)$
   5.1. Find a skeleton point *p* from *S*, and its minimum distance is $d_{\min}(p.q)$, where *q* is a skeleton point in *E*.
   5.2. Insert the skeleton arc into *E* and delete the skeleton from $\Re$.
6. While $(T \neq NULL)$
   6.1. Find a skeleton point p from T, and its minimum distance is $d_{\min}(p.q)$, where *q* is a skeleton point in *E*.
   6.2. Insert the skeleton branch into *E* and delete the skeleton point from T.

III. CONTOUR REPRESENTATION BASED ON TWO CONSECUTIVE PRIMITIVE EDGES

In the computer vision there is a long history of work on contour representation and contour similarity. Some well-known methods include Fourier descriptor, moment invariants, wavelet descriptors and histogram of boundary directors. Without loss of generality, the histogram of *CPE* in Eq.(3) is used to describe the contour representation in this paper. For practical purposes, the histogram of *CPE* method cannot efficiently and correctly described the contour of an object. As shown in Fig. 2(c) and (f), the histogram of *CPE* is the same because it is a discrete primitive visual pattern. To solve this problem, the Eq.(3) is modified into two consecutive primitive edge $\Gamma^{(\alpha)}$ as follows:

$$\Gamma^{(\alpha)} = \phi_j \cup \phi_{j+1} = |e_j - e_{j-1}| \cup |e_{j+1} - e_j| \text{ or}$$
$$\Gamma^{(\alpha)} = \phi_{j+1} \cup \phi_j = |e_{j+1} - e_j| \cup |e_j - e_{j-1}| \quad (21)$$

where $\cup$ denotes a union operation. Instead of representing a boundary in any possible combination, the detected two-consecutive primitive edge (*TCPE*) is mapped to 16 types of visual pattern as shown in Fig.5. The main reason for mapping the *TCPE* to virtual-pattern is to encode the boundary of an object with visual-pattern block by block along the edge pixels. Hence, two given object blocks from along the boundary pixel can be encoded and can indicate which visual-pattern is mapped. If we have a shape of an object such as Fig. 1, the *R*-table can be modified based on the proposed *TCPE* as

$$(\Gamma_1^\alpha, (a_0, a_1, a_2, a_3)), (\Gamma_2^\alpha, (a_2, a_3, a_4, a_5)), ..., (\Gamma_n^\alpha, (a_n, a_{n+1}, a_0, a_1)) \quad (22)$$

where α is belonging to the type of virtual-pattern in Fig. 5, a_0 and a_n denote the start-point and end-point respectively. To obtain the consistency of *TCPE* for any structure of objects, two decision rules are considered: (1) the starting boundary and ending boundary overlap; (2) the scanning sequence uses the anticlockwise method in the boundary of object.

IV. SIMILARITY MEASUREMENT OF OBJECT

REPRESENTATION

Consider a database *DB* consisting of a large number of objects. Each of them is represented as a high-dimensional feature vector $F=\{\Gamma,\Phi,\beta\}$, where Γ,Φ and β denote the feature vector of *TCPE*, skeleton arcs, and skeleton branch in an object, respectively. The feature vector of *TCPE* can further be represented as $\Gamma=\{\{f_i,p_j\},i=1,...,16;\ j=1,...,n\}$, where f_i and p_j are *i*th feature and the corresponding number of *TCPE* in Fig. 6, respectively. The total number of *TCPE* in an object can be computed as

$$\zeta=\sum_{i=1}^{16}p_{i,j}. \tag{23}$$

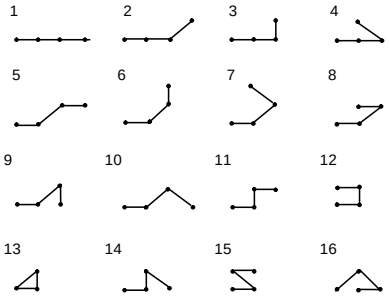

Fig.5. Possible sixteen types of visual patterns in a square block.

Let $X=\{\{x_i,p_k\},k=1,...,16\}$ and $Y=\{\{y_j,q_k\},k=1,...,16\}$ be the feature vectors of *TCPE*. Then the distance between *X* and *Y* based on the concept of QBIC [6] can be computed as

$$D_{TCPD}{}^2(x,y)=\sum_{i=1}^{16}p_i^2+\sum_{j=1}^{16}q_j^2-\sum_{i=1}^{16}\sum_{j=1}^{16}2a_{i,j}p_iq_j \tag{24}$$

where a_{ij} is the perceptual coefficient between feature values p_k and q_k. The role of each *TCPE* in any object is different from the sense of human vision. The fewer numbers of *TCPE* is more important than many numbers of *TCPE* in an object. Thus, the perceptual coefficient a_{ij} can be defined as

$$a_{i,j}=\frac{|\frac{1}{p_i}+\frac{1}{q_j}|}{\sum_{i=1}^{16}\sum_{j=1}^{16}|\frac{1}{p_i}+\frac{1}{q_j}|} \tag{25}$$

where the values p_i and q_j are assumed as non-zero, otherwise the corresponding value of $1/p_i$ or $1/q_j$ is assigned as zero.

The feature vector of skeleton arcs can further be represented as $\beta=\{\{s_i,s_{i+1},\theta_i\},i=1,...,n\}$ shown as Fig. 6, where s_i and s_{i+1} are the consecutive of skeleton arcs and θ_i denotes the included angle between the consecutive skeleton arcs s_i and s_{i+1}. A weight of skeleton arcs in an object can be found as

$$W^{sa}=\sum_{i=1}^{n}W_i^{sa} \tag{26}$$

and the W_i^{sa} is defined as

$$W_i^{sa}=\frac{\theta_i}{s_i+s_{i+1}} \tag{27}$$

Let $X=\{\{s_i^a,s_{i+1}^a,\theta_i^a\},i=1,...,n\}$ and $Y=\{\{s_j^b,s_{j+1}^b,\theta_j^b\},j=1,...,m\}$ be the feature vectors of skeleton arcs. Then the distance between *X* and *Y* is computed as

$$D^{sa}=|W_X^{sa}-W_Y^{sa}| \tag{28}$$

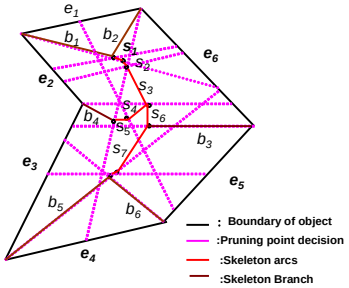

Fig. 6. An example of representing an object by the boundary of object, skeleton arcs, and skeleton branch.

The feature vector of a skeleton branch can further be represented as $\phi_1=\{\{e_i,e_j,b_k\},i,j=1,...,m,k=1,...,n\}$ shown as Fig. 6, where b_k denotes the skeleton branch, and e_i and e_j are the boundary edges of object, which is connecting to the skeleton branch b_k. A weight of a skeleton branch in an object can be found as

$$W^{sb}=\sum_{i=1}^{n}W_i^{sb} \tag{29}$$

and the W_i^{sb} is defined as

$$W_{b_k}^{sb}=\begin{cases}\frac{s_j}{s_i}, & when\quad s_i>s_j\\ \frac{s_i}{s_j}, & when\quad s_j>s_i\end{cases} \tag{30}$$

Let $X=\{\{e_i^x,e_j^x,b_k^x\},i,j=1,...,m_1,k=1,...,n_1\}$ and $Y=\{\{e_l^y,e_m^y,b_n^y\},l,m=1,...,m_1,n=1,...,n_1\}$ be the description vectors of a skeleton branch. Then the distance between *X* and *Y* is computed as

$$D^{sb}=|W_X^{sb}-W_Y^{sb}| \tag{31}$$

Note that the values of D_{TCPD}, D^{sb} and D^{sa} should be normalized by the maximum values of D_{TCPD}, D^{sb} and D^{sa} respectively before advancing to define similarity measurements between the two objects *X* and *Y*. This normalization process will result in the normalized values of D_{TCPD}, D^{sb} and D^{sa} are confined to be within the (0,1) interval. Let $\tilde{D}_{TCPD}$, $\tilde{D}^{sb}$ and $\tilde{D}^{sa}$ denote the normalized D_{TCPD}, D^{sb} and D^{sa}, respectively. The measurement of similarity $D_s(X,Y)$ between the two objects *X* and *Y* on the basis of skeleton arc and skeleton branch features are then defined as

$$D_s(X,Y)=1-(\alpha_1\cdot\tilde{D}^{sb}+\alpha_2\cdot\tilde{D}^{sa}) \tag{32}$$

where α_1 and α_2 represent the weighting of $\tilde{D}^{sb}$ and $\tilde{D}^{sa}$ respectively and $\alpha_1+\alpha_2=1$. Note that the value of $D_s(X,Y)$

between 0 and 1. The larger the value of $D_s(X,Y)$, mean a greater similarity between the query object X to the database object Y. Combining the skeleton and contour features, the hybrid similarity measurement can be defined as

$$D_{Total} = \beta_1 \cdot D_s(X,Y) + \beta_2 \cdot \tilde{D}_{TCPD} \qquad (33)$$

where D_{Total} is the value of hybrid similarity, $D_s(X,Y)$ and $\tilde{D}_{TCPD}$ are the values of similarity on the basis of skeleton and contour features respectively, and β_1 and β_2 represent the weighting of $D_s(X,Y)$ and $\tilde{D}_{TCPD}$, respectively. We should also set $\beta_1 + \beta_2 = 1$.

V. EXPERIMENTAL RESULTS

In order to evaluate the proposed approach, a series of experiments were conducted on an Intel PENTIUM-IV 3GHz PC. A skeletal measure method proposed by Torsello and Hancock's method [7] is also simulated by computer software for the purpose of performance comparison. An image database which consisted of 1266 binary objects is extracted from scenery images. Each object image in database is first formatted to 256×256 for testing the retrieval approach. Before the evaluation, human assessment was done to determine the relevant matches in the database to the query object image. The top 100 retrievals from both the Torsello and Hancock's method and the proposed approaches were marked to decide whether they were indeed visually similar in skeleton and contour.

It is difficult to derive a formal method in evaluating the retrieval accuracy of an image database system. Traditional metrics for evaluating performance are recall and precision. They are functions of both correct matches and the relevance of database images to a query. The retrieval accuracy measured by recall and precision is computed as following. Recall measures the ability of the system to retrieval all the images that are relevant and defined as

$$\text{Re}\,call = \frac{\text{Re}\,levances \quad correctly \quad retrieved}{all \quad relevances}.$$

Precision measures the ability of the system to retrieve only images that are relevant and can be computed by

$$\text{Pr}\,ecision = \frac{relevances \quad correctly \quad retrieved}{all \quad retrieved}.$$

Recall and precision require a ground truth to assess the relevance of images for a set of significant queries.

The performance of the proposed image retrieval method is evaluated in terms of retrieval accuracy. The average precision and recall curves are plotted in Figs. 7(a) and 7(b), respectively. It can be seen that the proposed method achieves good results in terms of retrieval accuracy compared with Torsello and Hancock's method [7].

VI. CONCLUSION

In this paper we have presented the recognition of shape-matching for object retrieval in image databases using skeleton and contour by discrete curve evaluation and two consecutive primitive edges. Object segmentation and recognition is the primary step of computer vision to achieve image retrieval of high-level image analysis. Contour-based and skeleton-based representations are important for object recognition in different areas. In this paper, we proposed a novel method to integrate the contour-based approaches with skeleton-based approaches for object representation. The contour-based and skeleton-based representations are based on the proposed two-consecutive primitive edges method and discrete curve evolution method respectively. The experimental results demonstrate that the proposed method is superior to Torsello and Hancock's method in terms of retrieval accuracy.

REFERENCES

[1]W. H. Tsai. And S. S. Yu, 1985, "Attributed string matching with merging for shape recognition," IEEE Trans. PAMI, 7(4), pp. 453-462.
[2] L. J. Latecki and R. Lakamper, 1999, "Convexity Rule for shape Decomposition Based on Discrete Contour Evolution," Computer Vision and Image Understanding, 73(3), pp. 441-454.
[3] C. D. Ruberto, 2004, "Recognition of shape by attributed skeletal graphs," Pattern Recognition, 37, pp. 21-31.
[4] S. C. Cheng, C. T. Kuo and H. J. Chen, 2007, "Visual object retrieval via block-based visual-pattern matching," Pattern Recognition, 40, pp. 1695-1710.
[5] L. J. Latecki and R. Lakamper, 1999, " Convexity Rule for Shape Decomposition Based on Discrete Contour Evolution," Computer Vision and Image Understanding, 73, pp.441-454.
[6] M. flickner, H. Sawhney, W. Niblack, J. Ashley, Q. Huang, B. Dom, M. Gorkani, J. Hafner, D. Lee, D. Petkovic, D. Steele, and P. Yanker," Query by image and video content: the QBIC system, IEEE Computer, 28(9), pp23-32, 1995.
[7] A. Torsello and E. R. Hancock, 2004," A Skeletal measure of 2D shape similarity," Computer Vision and Image Understanding, 95, pp. 1-29.

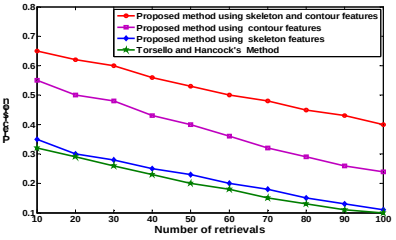

(a)

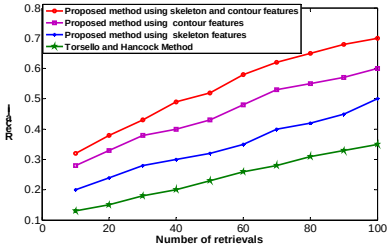

(b)

Fig.7. Average precision and recall versus number of retrieved image: (a) Precision; (b) Recall.